Journal of the Korean Society of Surveying, Geodesy, Photogrammetry and Cartography
Vol. 35, No. 5, 339-348, 2017
https://doi.org/10.7848/ksgpc.2017.35.5.339

ISSN 1598-4850(Print)
ISSN 2288-260X(Online)
Original article

Development of Image-based Assistant Algorithm for Vehicle Positioning by Detecting Road Facilities

Jung, Jinwoo[1] · Kwon, Jay Hyoun[2] · Lee, Yong[3]

Abstract

Due to recent improvements in computer processing speed and image processing technology, researches are being actively carried out to combine information from a camera with existing GNSS (Global Navigation Satellite System) and dead reckoning. In this study, the mathematical model based on SPR (Single Photo Resection) is derived for image-based assistant algorithm for vehicle positioning. Simulation test is performed to analyze factors affecting SPR. In addition, GNSS/on-board vehicle sensor/image based positioning algorithm is developed by combining image-based positioning algorithm with existing positioning algorithm. The performance of the integrated algorithm is evaluated by the actual driving test and landmark's position data, which is required to perform SPR, based on simulation. The precision of the horizontal position error is 1.79m in the case of the existing positioning algorithm, and that of the integrated positioning algorithm is 0.12m at the points where SPR is performed. In future research, it is necessary to develop an optimized algorithm based on the actual landmark's position data.

Keywords: Vehicle Positioning, Sensor Fusion, Single Photo Resection, Machine Learning, Object Detection, Road Facilities

1. Introduction

The existing vehicle positioning technology is utilized on navigation or ADAS (Advanced Driver Assistance System), which assists the driver by informing and automatically controlling the state of the vehicle based on the information obtained through various sensors attached to the vehicle. In recent days, it has been evaluated as an essential element for the development of an autonomous vehicle, so related research is actively under study. However, current commercial positioning technology operates on the basis of GNSS (Global Navigation Satellite System), which is sensitive to changes in the signal reception environment, so positioning can not be performed properly due to multi-path or signal blockage in closed-space, such as building forests or tunnels. In order to solve such problems, various institutes in Korea and abroad conduct research on dead reckoning, which determines relative position and attitude of the vehicle by integrating the acceleration and angular velocity obtained from various sensors such as IMU (Inertial Measurement Unit), but there is a problem that positioning accuracy is reduced exponentially due to accumulation of the sensor error if GNSS signal blockage is prolonged.

Recently, as the development of computer and an image

Received 2017. 09. 25, Revised 2017. 10. 10, Accepted 2017. 10. 22
1) Member, Dept. of Geoinformatics, Univ. of Seoul (E-mail: jw_jung@uos.ac.kr)
2) Corresponding Author, Member, Dept. of Geoinformatics, Univ. of Seoul (E-mail: jkwon@uos.ac.kr)
3) Member, Dept. of Geoinformatics, Univ. of Seoul (E-mail: acce00@uos.ac.kr)

sensor, it is possible to process the image in real time, and studies are actively conducted to utilize in positioning field. Nistér *et al*. (2006) used visual odometry to determine the relative position of the vehicle using motion vector generated by extracting and matching feature points between consecutively received image frames, but position accuracy is reduced as the running time goes and it is impossible to be operated in an area in which feature can not be extracted sufficiently. Kim and Park (2014) used the stereo camera, which calculates the distance between the specific object using disparity to determine the camera position, but it requires costly inefficiency because two cameras must be operated. Habib *et al*., (2000) used SPR (Single Photo Resection) and mono camera to determine position and attitude of the camera. SPR is based on the collinear condition that coordinates of the specific object in ground coordinate system, the center of lens and the coordinates of the object in image coordinate system are located on a common line. Therefore, it is possible to directly determine the position of the camera, and it only operates one camera.

In this study, image-based assistant algorithm for vehicle positioning is developed using SPR considering economical aspect and performance, and factors affecting SPR are analyzed based on simulation test. In addition, GNSS/on-board vehicle sensor/image based positioning algorithm, which is robust to driving environment changes, is developed by combining with the previously developed GNSS/on-board vehicle sensor based positioning algorithm. The performance of the integrated positioning algorithm is evaluated by generating the position of the road facilities on the basis of the simulation based on the assumption that the road facility position DB (Data Base) is constructed.

2. Image-based Assistant Algorithm for Vehicle Positioning

2.1 Mathematical model

SPR, which is a mathematical model of the image-based assistant algorithm for vehicle positioning, uses the collinear condition that image coordinates and ground coordinates of the specific object and center of lens are located on common line (Fig. 1 and Eq. (1)).

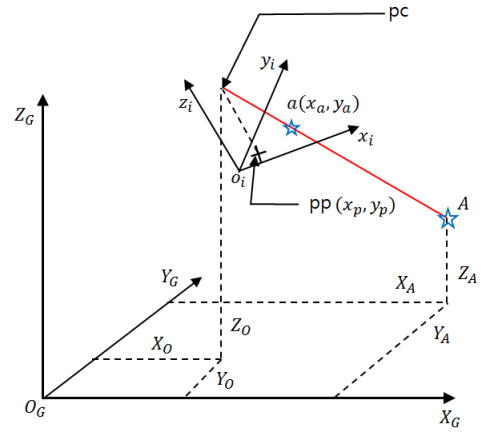

Fig. 1. Collinear condition between image coordinates 'a' and object coordinates 'A'

$$x_a = x_p - c\frac{r_{11}(X_A - X_O) + r_{12}(Y_A - Y_O) + r_{13}(Z_A - Z_O)}{r_{31}(X_A - X_O) + r_{32}(Y_A - Y_O) + r_{33}(Z_A - Z_O)}$$
$$y_a = y_p - c\frac{r_{21}(X_A - X_O) + r_{22}(Y_A - Y_O) + r_{23}(Z_A - Z_O)}{r_{31}(X_A - X_O) + r_{32}(Y_A - Y_O) + r_{33}(Z_A - Z_O)} \quad (1)$$

where, (x_a, y_a) : image coordinates of point A

(x_p, y_p) : calibrated principal point position

c : focal length of camera

$r_{11}, r_{12}, \cdots, r_{33}$: elements of the rotation matrix R

(X_A, Y_A, Z_A) : object coordinates of point A

(X_O, Y_O, Z_O) : object coordinates of perspective center

In order to perform SPR, the collinear equation formula is linearized with respect to the position (X_O, Y_O, Z_O) and attitude (ϕ, θ, ψ), which is EO (Exterior Orientation) of the camera. The linearized collinear equation is expressed as Eq. (2), since the component of the rotation matrix is represented by the attitude of the camera.

$$\begin{bmatrix} x_a - (x_a)^0 \\ y_a - (y_a)^0 \end{bmatrix} = \begin{bmatrix} \frac{\partial x_a}{\partial X_0} & \frac{\partial x_a}{\partial Y_0} & \frac{\partial x_a}{\partial Z_0} & \frac{\partial x_a}{\partial \phi} & \frac{\partial x_a}{\partial \theta} & \frac{\partial x_a}{\partial \psi} \\ \frac{\partial y_a}{\partial X_0} & \frac{\partial y_a}{\partial Y_0} & \frac{\partial y_a}{\partial Z_0} & \frac{\partial y_a}{\partial \phi} & \frac{\partial y_a}{\partial \theta} & \frac{\partial y_a}{\partial \psi} \end{bmatrix} \begin{bmatrix} dX_0 \\ dY_0 \\ dZ_0 \\ d\phi \\ d\theta \\ d\psi \end{bmatrix} \quad (2)$$

Two equations are established through one image coordinate defined in two-dimensional space. Therefore, it is necessary to extract at least three image coordinates in order to estimate six unknowns, which is position and attitude in three-dimensional space.

2.2 Road facilities detection algorithm

2.2.1 Object detection based on machine learning

Object detection based on machine learning is performed by a process of extracting data from an input image and classifying the data to determine if the data is the target to be detected (positive) or not (negative). The data extracted from the image is called feature. In this study, HOG (Histogram of Oriented Gradient) feature is used, and it extracts information about the shape of an object by calculating gradient, which is a derivative of brightness, and generating histogram according to a direction of the gradient.

The input image is divided into cells defined by the size of a certain pixel, and a histogram is generated in this defined unit. The direction of the calculated gradient is classified into nine histogram bins at intervals of 40° based on 360°. Then, the magnitude of the calculated gradient is defined as the value of the histogram corresponding to the direction. The histogram extracted in the unit of cells is configured as a feature vector in blocks, which is defined by the size of a certain cell, and this process is illustrated in Fig. 2.

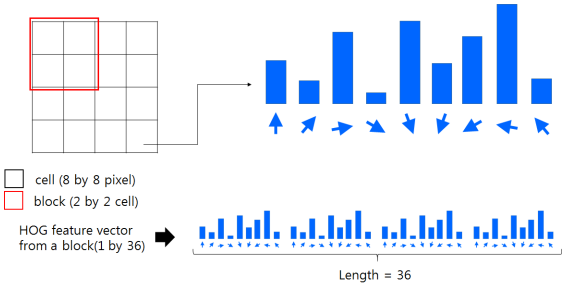

Fig. 2. HOG feature extraction in blocks

HOG features classified by the positive, the target to be detected through data classification, otherwise the negative cases. This process is done through a pre-learned classification model through a large amount of training data. In this study, a road facilities detection algorithm is implemented by combining two methods, AdaBoost (Adaptive Boosting) and SVM (Support Vector Machine), which are typically applied in the field of machine learning.

AdaBoost linearly combines weak classifiers that classify data according to a simple criterion to create a strong classifier with one complex criterion (Dalal and Triggs, 2005). AdaBoost has a merit that it has a fast execution speed since the next weak classifier is no longer applied in the region rejected by the initial weak classifier in the process of applying to the image, and it is shown in Fig. 3 (Viola and Jones, 2004). Therefore, AdaBoost is used to extract candidates to detect quickly.

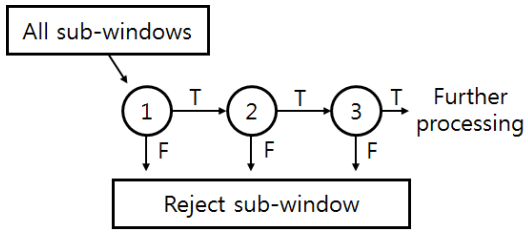

Fig. 3. Process of several weak classifiers

SVM classifies data by generating a hyperplane in a multidimensional space in which extracted features exist (Theodoridis and Koutroumbas, 2008). It has the advantage of being able to sort correctly when receiving new input data since the hyperplane is determined by the mathematical conditions that determine support vector, which is the closest vector, and maximize the margin between the two groups to be classified. Thus, SVM is applied to detect the final road facilities according to detailed standards which come from the candidates detected through AdaBoost. Fig. 4 represents the process of classifying the positive group which is the detection of desired targets, and the negative group through the SVM.

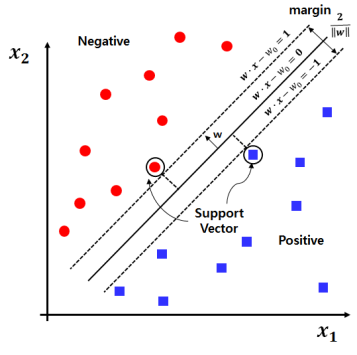

Fig. 4. Hyperplane separates between positive and negative classes

2.2.2 Development of road facilities detection algorithm

Road facilities detection algorithm is developed using object detection based on machine learning. Road facilities to be detected are selected as road signs, traffic lights, and road surface marking considering the actual driving environment and the conditions that at least 3 reference points need to be extracted to perform SPR. In this regard, the image reference point used for SPR is defined as the center point of the detected road facilities.

Fig. 5. Sample image of road sign

In the case of road signs, street-name address based signs are selected, and Fig. 5 is the sample image. Since the street-name address based sign has the feature that it contains left and right direction arrows inside the rectangle shape, the candidates of the road sign having rectangle shape are extracted by using the classification model learned based on AdaBoost. Using the SVM-based model for the extracted candidates, the arrows with the left and right directions inside the sign are detected, and the candidate group including the arrows in both directions is finally selected as the road sign.

In order to detect a traffic light, a candidate group with a rectangular shape of a traffic light is extracted using an AdaBoost-based model, and a circular shape corresponding to a lamp inside the traffic light is detected by applying an SVM-based model. Fig. 6 shows an example of a traffic light to be detected.

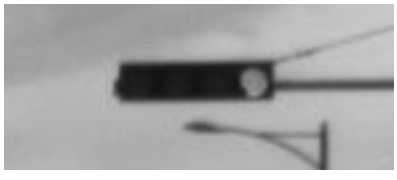

Fig. 6. Sample image of traffic light

The types of road surface marking installed in the actual driving environment are various. Thus, in this study, we present seven types of road mark which are installed in Daegu Technopolis district, and it is shown in Fig. 7.

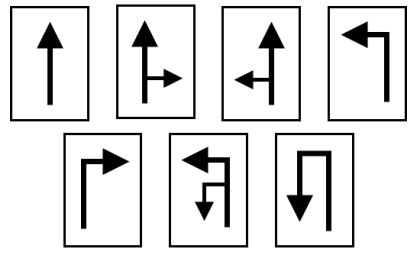

Fig. 7. Seven types of road surface marking to detect

Since the road surface marking is characterized by its shape changing according to the distance from the vehicle, it transforms part of the image acquired through the front camera as if it is seen in the air. To do this, IPM (Inverse Perspective Mapping) developed by Eric and Randy (2007) is applied. The results are shown in Fig. 8.

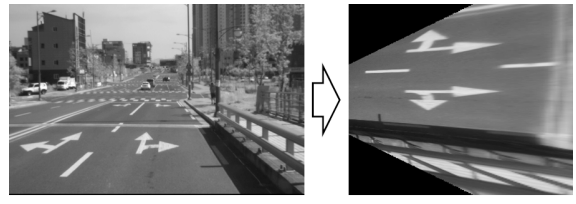

Fig. 8. Input image (left) and IPM image (right)

After performing the IPM, lane corresponding to a straight line component is detected and set as ROI (Region Of Interest) for detection. At this point, hough transform, which transforms a two-dimensional image space to a parameter space for a straight line, is applied for lane detection. Pre-learned SVM model is applied for detecting the seven types

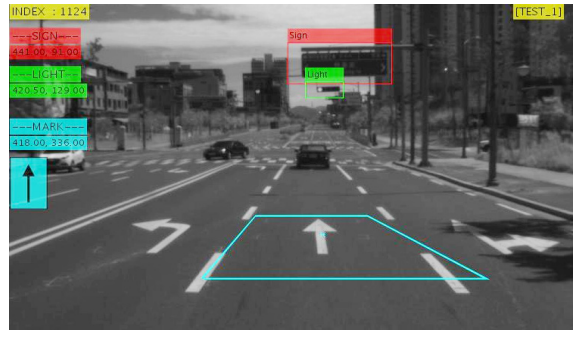

Fig. 9. Sample image of the point where SPR can be performed

of road surface marking mentioned above for the ROI.

For the development of the road facilities detection algorithm, the training data is obtained by 10 times of driving for about 250 minutes in Daegu Technopolis district. Fig. 9 is an example of the point in which SPR can be performed by extracting three or more reference points in one frame.

3. Development of GNSS/on-board Vehicle Sensor/image Based Positioning Algorithm

GNSS/on-board vehicle sensor/image based positioning algorithm is developed by combining image-based positioning algorithm with existing positioning algorithm developed by Han (2016) to determine continuous and stable vehicle position. Han (2016) developed dead reckoning system based on WSS (Wheel Speed Sensor), YRS (Yaw Rate Sensor), GS (Gravity Sensor). In addition, position and velocity determined through GNSS are loosely coupled with the dead reckoning system based on EKF (Extend Kalman Filter) to compensate the error. The error state vector consists of 13 components as can be seen in Eq. (3). The state vector of navigation error (δx_{NAV}) consists of position error ($\delta\varphi$, $\delta\lambda$, δh), velocity error in NED frame (δv_n, δv_e, δv_d), attitude error ($\delta\phi$, $\delta\theta$, $\delta\psi$). The state vector of sensor error (δx_{SENSOR}) consists of WSS scale factor (δs_v), YRS bias (δb_{YRS}), GS bias ($\delta b_{x,GS}$, $\delta b_{y,GS}$).

$$\delta x_{WSS/YRS/GS} = \begin{bmatrix} \delta x_{NAV} \\ \delta x_{SENSOR} \end{bmatrix} \tag{3}$$

where, δx_{NAV} : state vector of navigation error
($\delta x_{NAV} = [\delta\varphi\ \delta\lambda\ \delta h\ \delta v_n\ \delta v_e\ \delta v_d\ \delta\phi\ \delta\theta\ \delta\psi]^T$)

δx_{SENSOR} : state vector of sensor error
($\delta x_{SENSOR} = [\delta s_v\ \delta b_{YRS}\ \delta b_{x,GS}\ \delta b_{y,GS}]^T$)

The position and attitude of the vehicle determined by the dead reckoning system are used as the initial EO to perform SPR, and EO calculated by SPR is used to compensate the error of the dead reckoning system. Eq. (4) represents the observation equation to update the state vector.

$$z_{SPR} = H_{SPR} \cdot x(t) + v_{SPR}, v_{SPR} \sim (0, R_{SPR}) \tag{4}$$

Eq. (5) represents the indirect observation, which is the difference of the estimation between the dead reckoning system and SPR. Eq. (6) is the design matrix, and Eq. (7) is the variance-covariance matrix.

$$z_{SPR} = \begin{bmatrix} \varphi \\ \lambda \\ h \\ \phi \\ \theta \\ \psi \end{bmatrix}_{WSS/YRS/GS} - \begin{bmatrix} \varphi \\ \lambda \\ h \\ \phi \\ \theta \\ \psi \end{bmatrix}_{SPR} \tag{5}$$

$$H = \begin{bmatrix} I_{3\times3}\ 0_{3\times3}\ 0_{3\times3}\ 0_{3\times4} \\ 0_{3\times3}\ 0_{3\times3}\ I_{3\times3}\ 0_{3\times4} \end{bmatrix} \tag{6}$$

$$R_{SPR} = diag\left(\left[\sigma_\varphi^2\ \sigma_\lambda^2\ \sigma_h^2\ \sigma_\phi^2\ \sigma_\theta^2\ \sigma_\psi^2\right]\right) \tag{7}$$

where, σ_φ^2 : variance of estimated latitude
σ_φ^2 : variance of estimated longitude
σ_h^2 : variance of estimated ellipsoidal height
σ_ϕ^2 : variance of estimated roll angle
σ_θ^2 : variance of estimated pitch angle
σ_ψ^2 : variance of estimated yaw angle

Fig. 10 shows a diagram of GNSS/on-board vehicle sensor/image based positioning algorithms. In this regard, the position and velocity from GNSS are loosely coupled to update the state vector.

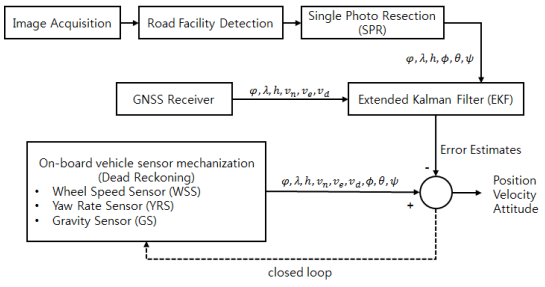

Fig. 10. Diagram of GNSS/on-board vehicle sensor/image based positioning algorithms

4. Performance Evaluation

4.1 Simulation tests for analyzing performance of SPR

Simulation test is performed in order to analyze the performance of SPR adopted as a mathematical model of the image-based assistant algorithm for vehicle positioning. The simulation data is generated based on POSLV data, which is assumed to be the true value in this study with precision of cm-level. In this regard, the additional error is generated

for each test to generate final simulation data. 100 position and attitude data are extracted from POSLV data obtained from the actual driving at the same interval, and it is assumed to be the true EO, which is the position and attitude of the camera. The simulation data is generated by generating a collinear line between the camera and the previously defined IP (Image Point) and determining the position of the GCP (Ground Control Point). Tests are conducted to analyze the effect of 1) the precision of GCP position, 2) the precision of initial EO and 3) geometry of IP.

The geometry of IP is classified into 6 types. Type 1 is wide spread, type 2 is narrow in horizontal, type 3 is narrow in vertical, and type 4 is narrow in all directions. Type 5 and 6 are assumed to be the actual point where SPR is performed. Type 5 is the case in which traffic sign, traffic light and road surface marking are detected, and type 6 is the case in which traffic sign and two traffic lights are detected. The distance between the camera and each GCP corresponding to each image is summarized in Fig. 11, and type 1 to type 4 are same.

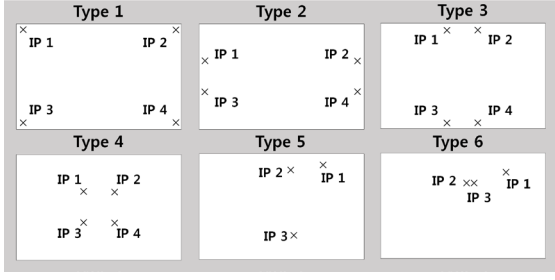

(unit : m)

	Type 1	Type 5	Type 6
IP 1	15	55	55
IP 2	10	50	45
IP 3	10	10	50
IP 4	15	-	-

Fig. 11. Types of IP and distance between camera and GCP

The error is defined as the difference between EO of the camera calculated after SPR performed and POSLV, and RMSE (Root Mean Square Error) is expressed in a graph. Position is expressed with respect to the body frame consists of the moving direction (X axis), the right direction of the moving direction (Y axis) and down direction (Z axis). Attitude is expressed by roll, pitch and yaw.

Tests to analyze the precision of GCP position are performed with the condition that initial EO error is 1m and 1° considering the performance of positioning algorithm, and geometry of IP is type 1. As can be seen in Fig. 12, RMSE of 0m case is very close to zero. However, as the position error of GCP increases, position and attitude error increases, and horizontal error is 0.7m and vertical error is 0.5m when the error of GCP is 0.2m. In other words, SPR performance is reliable when GCP position is very precise, but about 2° attitude error occurs in violation of the collinear condition if the precision of GCP position is 0.2m level.

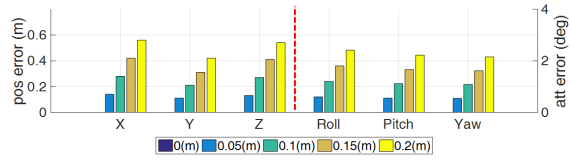

Fig. 12. RMSE of GCP test (Type 1)

Tests to analyze the precision of initial EO are performed with the condition that precision of GCP position is 0.15m, and geometry of IP is type 1. As can be seen in Fig. 13, SPR performance is similar until initial EO error is 5m, 1.5°. However, the error increases sharply when initial EO error is 10m, 3°. That is, if reliable GCP position DB is constructed, SPR eliminates cumulative error in GNSS blockage area.

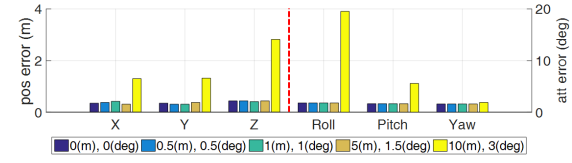

Fig. 13. RMSE of EO test (Type 1)

Tests to analyze the geometry of IP is divided into 1) tests based on a distance between the camera and GCP 2) tests based on various types of IP geometry. Firstly, tests based on distance between camera and GCP are performed with the condition that geometry of IP is type 1, initial EO error is 1m and 1°, and a distance between the camera and each GCP corresponding to IP 2 and 3 is fixed to 10m, and IP 1 and 4 is set to 10m, 15m, 20m, 30m and 50m, respectively. The precision of GCP position is set to 0.15m. As can be seen in Fig. 14, the larger the distance differences, the smaller

the overall error. This is because independence among each observation is ensured. In addition, estimated attitude is precise when the distance is large, because the GCP is located close to the collinear line with the same GCP position error (0.15m).

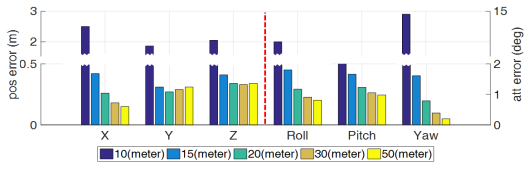

Fig. 14. RMSE of depth test (Type 1)

Tests based on various kinds of IP geometry are performed by every type of IP in Fig. 11. Tests are performed with the condition that GCP position error is 0.15m, initial EO error is 1m and 1°. As can be seen in Fig. 15, it can be seen that as the IP converges, the geometry is unstable and error tends to increase from type 1 to 4. Especially, roll and pitch error is about 4°, which is larger than others. Type 5 and 6, assuming the actual point where SPR is performed, show reliable results in type 5 because of the stable geometry. Yaw is determined more precisely, because of a difference in distance between GCP. In addition, the reason why the error of roll and pitch is larger than yaw is based on the facts that GCP is concentrated in the front direction of the lens.

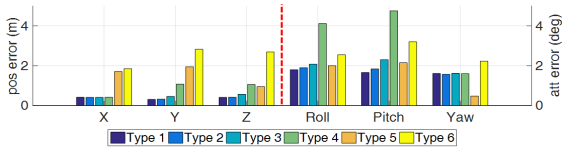

Fig. 15. RMSE of geometry test

4.2 Performance evaluation of GNSS/on-board vehicle sensor/image based positioning algorithm

The driving test is performed to evaluate the performance of GNSS/on-board vehicle sensor/image based positioning algorithm. The driving route is selected considering the location of road facilities installed in Daegu Technopolis district. Fig. 16 shows the route in the north and south direction on the basis of the starting point, and 8 points where SPR is performed as a result of road facilities detection algorithm. The driving is carried out for about 20 minutes including stopping time before starting.

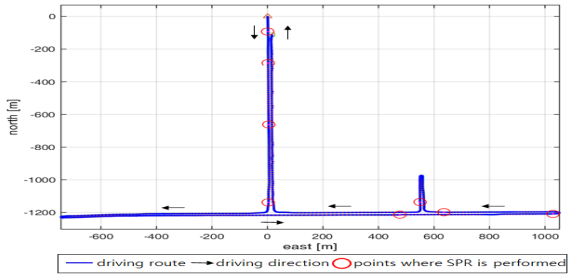

Fig. 16. Driving route and the points where SPR is performed (unit : m)

GNSS, on-board vehicle sensor and image data are obtained from actual driving. GCP position is generated based on simulation on the assumption that precise GCP position DB is constructed, and the distance between the camera and the reference points follows type 5 and type 6 in Fig. 11.

The performance evaluation of GNSS/on-board vehicle sensor/image based positioning algorithm is implemented by comparing with the existing GNSS/on-board vehicle sensor based positioning algorithm. The error is determined by comparing with POSLV data, and Table 1 and Table 2 summarize mean and standard deviation of the position and attitude error for the whole driving route. In this regard, the position error is expressed in body frame.

Table 1. Compared mean and standard deviation of position error (unit : m)

Parameter		GNSS/ on-board	GNSS/ on-board/Image
mean	X	0.51	0.36
	Y	-0.10	-0.10
	Z	0.00	-0.02
std	X	1.63	1.49
	Y	1.54	1.48
	Z	1.82	1.51

Table 2. Compared mean and standard deviation of attitude error (unit : deg)

Parameter		GNSS/ on-board	GNSS/ on-board/Image
mean	Roll	-0.36	-0.36
	Pitch	-0.30	-0.30
	Yaw	0.48	0.48
std	Roll	1.01	1.01
	Pitch	0.79	0.79
	Yaw	0.97	0.97

In the case of the position error, the precision of the X, Y, Z axis has improved, and mean of horizontal position error decreases from 0.52m to 0.37m. In the case of the attitude, none changes happen, because the correction of the attitude error is performed by SPR, but it is sharply returned to the original error size after SPR.

In order to analyze the effect of SPR for the whole driving, the horizontal error distribution is expressed in Fig. 17. The error is corrected by SPR performed, but it is rapidly returned to the original size of the error. Therefore, it is considered to perform optimal error modeling considering the relation between image-based algorithm for vehicle positioning and dead reckoning system.

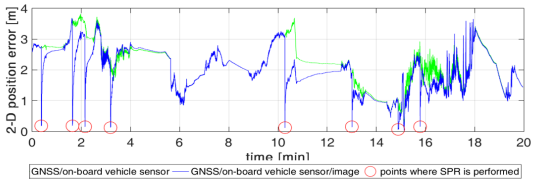

Fig. 17. Compared horizontal position error (unit : m)

The effect of SPR itself is analyzed by comparing the error between the two positioning algorithms at 8 points where SPR is performed. Table 3 and Table 4 summarize mean and standard deviation of the position and attitude error.

Table 3. Compared mean and standard deviation of position error at the points where SPR is performed (unit : m)

Parameter		GNSS/ on-board	GNSS/ on-board/Image
mean	X	2.08	-0.10
	Y	-0.14	-0.03
	Z	-0.34	0.00
std	X	1.18	0.07
	Y	1.34	0.10
	Z	2.55	0.00

Table 4. Compared mean and standard deviation of attitude error at the points where SPR is performed (unit : deg)

Parameter		GNSS/ on-board	GNSS/ on-board/Image
mean	Roll	-0.57	-0.00
	Pitch	-0.13	-0.00
	Yaw	0.58	0.02
std	Roll	0.56	0.00
	Pitch	1.39	0.00
	Yaw	0.48	0.01

The mean and standard deviation of the position and attitude errors are clearly reduced. The standard deviation of the horizontal position error decreases from 1.79m to 0.12m, and the performance improvement rate is 93%. The standard deviation of the yaw error decreases from 0.48° to 0.01°, and the performance improvement rate is 98%.

The position of GCP is generated based on simulation method without the error, so the performance of the algorithm would be degraded if actual data used. However, if precise GCP position DB and road facilities are constructed, it can be used to directly remove cumulative error due to disconnection of GNSS. In addition, this study has significance in which it can be used as an underlying research to develop the algorithm of the commercialization stage in the future.

5. Conclusion

The limitation and improvement plan of the road facilities detection algorithm and image-based assistant algorithm for vehicle positioning is proposed.

In the case of the road facilities detection algorithm, a monochrome camera is operated, so it is limited to determine the exact center of the object. Therefore, if the color camera is operated, these limitations can be resolved.

As a result of the simulation test to analyze the factors affecting SPR, the performance of SPR could be degraded according to the precision of GCP position and geometry of IP. It is considered to construct precise GCP position DB and install additional road facilities to obtain stable geometry of reference points.

The simulation test to evaluate the performance of GNSS/ on-board vehicle sensor/image based positioning algorithm is performed. The performance improvement rate of the precision of the horizontal position is 93%, and that of the yaw is 98%, so it is confirmed that the position and attitude error is eliminated at the points where SPR performed. However, there is a problem that the error increases sharply after SPR, so optimal error modeling should be performed considering the relation between the dead reckoning system and the image-based positioning system. In addition, it is confirmed that roll and pitch are relatively sensitive to the precision of GCP position as a result of the simulation test,

so it is considered to use the only yaw when updating the attitude in the development of the algorithm for practical use in the future.

Acknowledgments

This research was supported by Basic Science Research Program through the National Research Foundation of Korea (NRF) funded by the Ministry of Education (NRF-2015R1D1A1A01061319).

References

Dalal, N. and Triggs, B. (2005), Histograms of oriented gradients for human detection, *Proceedings of the CVPR 2005*, IEEE, 20-25 June, San Diego, California, Vol. 1, pp. 886-893.

Eric, J. and Randy H. (2007), Computer vision class project, *University of Utah*, Utah, http://www.eng.utah.edu/~hamburge/ (last date accessed: 18 September 2017).

Habib, A., Asmamaw, A., Kelley, D., and May, M. (2000), *Linear Features in Photogrammetry*, Report 450, Division of Geodetic Science, Ohio State University, Columbus, Ohio, pp. 9-21.

Han, J. H. (2016), *Performance Analysis of Positioning through the Integration of GNSS and On-board Vehicle Sensors*, Ph.D. dissertation, University of Seoul, Seoul, Korea, 165p.

Kim, N. H. and Park, C. H. (2014), Horizontal error analysis of stereo vision positioning system, *HCI KOREA 2015*, The HCI Society of Korea, 10-12 December, Seoul, Korea, pp. 24-26.

Nistér, D., Naroditsky, O., and Bergen, J. (2006), Visual odometry for ground vehicle applications, *Journal of Field Robotics*, Vol. 23, No. 1, pp. 3-20.

Theodoridis, S. and Koutroumbas, K. (2008), *Pattern Recognition 4th edition*, Academic Press, Cambridge, Massachusetts.

Viola, P. and Jones, M. J. (2004), Robust real-time face detection, *International Journal of Computer Vision*, Vol. 57, No. 2, pp. 137-154.